Characteristics of AOT Microemulsion Structure Depending on Apolar Solvents

ARTICLE *in* THE JOURNAL OF PHYSICAL CHEMISTRY B · OCTOBER 1999

Impact Factor: 3.3 · DOI: 10.1021/jp991899d

Characteristics of AOT Microemulsion Structure Depending on Apolar Solvents

Mitsuhiro Hirai,*,† Rika Kawai-Hirai,‡ Miwa Sanada,† Hiroki Iwase,† and Shingo Mitsuya†

Department of Physics, Gunma University, Maebashi 371-8510, Japan, and Meiwa Women's Junior College, Maebashi, Gunma 371, Japan

Received: June 10, 1999

By using synchrotron radiation small-angle X-ray scattering (SR-SAXS), we have studied the structural properties of reversed micellar systems depending on hydrocarbon chains of apolar solvents, where we have treated water/bis(2-ethylhexyl)sulfosuccinate (AOT)/*n*-hexane, *n*-heptane, *n*-octane, and isooctane systems. With increasing water/surfactant molar ratio w_0 (= $[H_2O]/[AOT]$), we have found that three different phases (oligomeric phase, transient phase, monomeric phase) appear successively in the above systems the same as in the water/AOT/isooctane system. In the present experiments we have found other features of the reversed micellar structure depending on apolar solvents. Thus, the w_0 region of the transient phase broadens with increasing the hydrocarbon chain length. The slope of the linear relation between micellar radius and w_0 changes systematically depending on the length of linear hydrocarbon chain of apolar solvent, which clearly suggests that the penetration of the solvent molecules into the surfactant layer of the micelle greatly depends on the length of the linear hydrocarbon chain. According to the systematic difference of the above slope from 1.5, where 1.5 is a well-known value obtained from geometrical constraint of micellar packing, we can estimate the penetration limit of apolar solvent with linear hydrocarbon chain to be $C_{9.5}$; therefore, over $C_{9.5}$ the penetration of apolar solvent molecules would hardly occur.

Introduction

Enzymes entrapped in water in oil (w/o) microemulsions are known to show significant enhancement of enzymatic activity, so-called super-activity, which has attracted significant interest concerning not only the biophysical catalytic properties of enzymes but also the possible future practical applications such as microreactors.[1−6] Previously, by using synchrotron radiation small-angle X-ray scattering (SR-SAXS) and enzymatic activity measurements we showed that the hydrolysis of some esters catalyzed by α-chymotrypsins entrapped in water/sodium bis-(2-ethylhexyl)sulfosuccinate (AOT)/isooctane reversed micelles is enhanced at low water/surfactant molar ratio w_0 (= $[H_2O]/[AOT]$) of 8−16 and that at this low w_0 range the appearance the oligomeric phase of the reversed micelle would play an important role for the acceleration of the metabolic turnover.[7,8] For water/AOT/hexane and water/AOT/heptane systems, our recent small-angle neutron scattering (SANS) experiments using a solvent contrast variation method clarified a change of the excluded volume of AOT molecule at low w_0 value which resulted in the increase of an apparent interfacial area of the micelles close to the enzymes.[9] In addition, our neutron spin−echo (NSE) study of the water/AOT/heptane system showed that the effective diffusion coefficient D_{eff} relating to bending fluctuation of the reversed micelle is significantly enhanced at low w_0 value.[10] These previous studies suggest that the structure and dynamics of the AOT-reversed micelles would be essentially important to the appearance of super-activity of enzymes entrapped in the reversed micelles. We have carried out further SR-SAXS experiments to clarify and compare the structural features of the AOT-reversed micelles with four different apolar solvents depending on w_0.

Experimental Section

Sample Preparation. Sodium bis(2-ethylhexyl)sulfosuccinate (AOT) was purchased from Nacalai Tesque Inc. Apolar solvents used were 98+ % *n*-hexane, 98+ % *n*-heptane, and 98+ % *n*-octane with infinity pure grade, and 99+ % isooctane, which were purchased from Wako Pure Chemical Industries Ltd. Water purified by a Millipore system was used. The reversed micellar solutions were obtained by using an injection method. The water contents in the reversed micellar solutions were determined by the Karl Fischer method using Metrohm 684 KF Coulometer. The water−surfactant molar ratios w_0 were 0, 4, 8, 12, 16, 20, 25, 30, 40, and 50. The AOT concentrations were 0.1 M.

Small-Angle Scattering Measurements and Data Analyses. Small-angle X-ray scattering (SAXS) experiments were carried out by using a SAXS spectrometer installed at the synchrotron radiation source (PF) at the High Energy Accelerator Research Organization (KEK), Tsukuba, Japan.[11] A one-dimensional position-sensitive proportional counter detected scattering intensities. Sample solutions were contained in mica window cells with 2 mm path length, whose cells were placed in a cell holder controlled at 25 °C. The X-ray wavelength used was 1.49 Å. The exposure time was 300 s for each sample.

The following standard analyses were executed. By using the Guinier plot ($\ln I(q)$ versus q^2) on the data sets in a defined small q range (0.02−0.03 $Å^{-1}$), we determined the values of both zero-angle scattering intensity $I(0)$ and gyration radius R_g by using the following equation

$$I(q) = I(0) \exp(-q^2 R_g^2/3) \quad (1)$$

* Address correspondence to: Mitsuhiro Hirai, Ph.D. Professor, Department of Physics, Gunma University, 4-2 Aramaki, Maebashi 371-8510, Japan. Fax: INT+81 272-20-7551 or 7552. Phone: INT+81 272-20-7554. E-mail: hirai@sun.aramaki.gunma-u.ac.jp.

† Gunma University.

‡ Meiwa Women's Junior College.

10.1021/jp991899d CCC: $18.00
Published on Web 10/14/1999

where $q = (4\pi/\lambda)\sin(\theta/2)$, θ and λ, are the scattering angle and the X-ray wavelength. The distance distribution function $p(r)$ was obtained by Fourier transform of the scattering intensity $I(q)$ as

$$p(r) = \frac{1}{2\pi^2}\int_0^\infty rq/(q)\sin(rq)\,dq \quad (2)$$

The $p(r)$ function depends both on the particle geometry and on the inner heterogeneity of the scattering density distribution in the particle. To calculate the function $p(r)$, extrapolation for the small-angle data sets was done by using the Guinier plot and the modified intensity as

$$I'(q) = I(q)\exp(-kq^2) \quad (3)$$

Here, k, the artificial damping factor, was used to remove the Fourier truncation effect. The radius of gyration of solute particles was determined by using the following equation given as

$$R_g^2 = \frac{\int_0^{D_{max}} p(r)r^2\,dr}{2\int_0^{D_{max}} p(r)\,dr} \quad (4)$$

where D_{max} is the maximum diameter of the particle and was estimated from the $p(r)$ function satisfying the condition $p(r) = 0$ for $r > D_{max}$.[12]

Results and Discussion

Figure 1 shows the w_0 dependence of the scattering curves $I(q)$ of the water/AOT/*n*-hexane, water/AOT/*n*-heptane, and water/AOT/*n*-octane systems, where (a), (b), and (c) correspond to the above different reversed micellar solutions, respectively. In Figure 1 the AOT concentration is 0.1 M. With increasing w_0 value, the scattering intensities in the small q region increase. These changes of the scattering curves well reflect an enlargement of the micellar dimension with increasing water pool radius.

Figure 2 shows the distance distribution functions $p(r)$ obtained by using eq 2 for the scattering curves in Figure 1. For all apolar solvents, at $w_0 = 0$ the $p(r)$ function shows a symmetric bell-shaped peak profile. With increasing water content, the bell-shaped peak profile accompanies a low hump or a shoulder. At higher water content such a low hump or a shoulder disappears and the $p(r)$ function turns to show again a symmetric bell-shaped profile. The shift of the peak position of the $p(r)$ function evidently indicates an enlargement of the micellar dimension with increasing water pool radius, as also suggested by the change of the scattering curves in Figure 1. In addition, the positions of the low humps or the shoulders mostly locate twice or thrice distance compared with the positions of the first maximums in the $p(r)$ functions. Then, the appearance of the low hump or the shoulder is attributable to the presence of oligomeric particles such as dimer or trimer.[8,13,14] The above changing tendency of the $p(r)$ function is essentially the same for all systems; however, the extent of the appearance of the low hump and the w_0 region with the low hump differ from one another for the three apolar solvents. Thus, with increasing the hydrocarbon chain length of solvent, the low-hump w_0 region broadens and the hump profile becomes more evident.

By using eq 4 we can estimate the water content dependence of the radius of gyration R_g of the w/o AOT droplets, which is shown in Figure 3. Evidently, for each apolar solvent we can

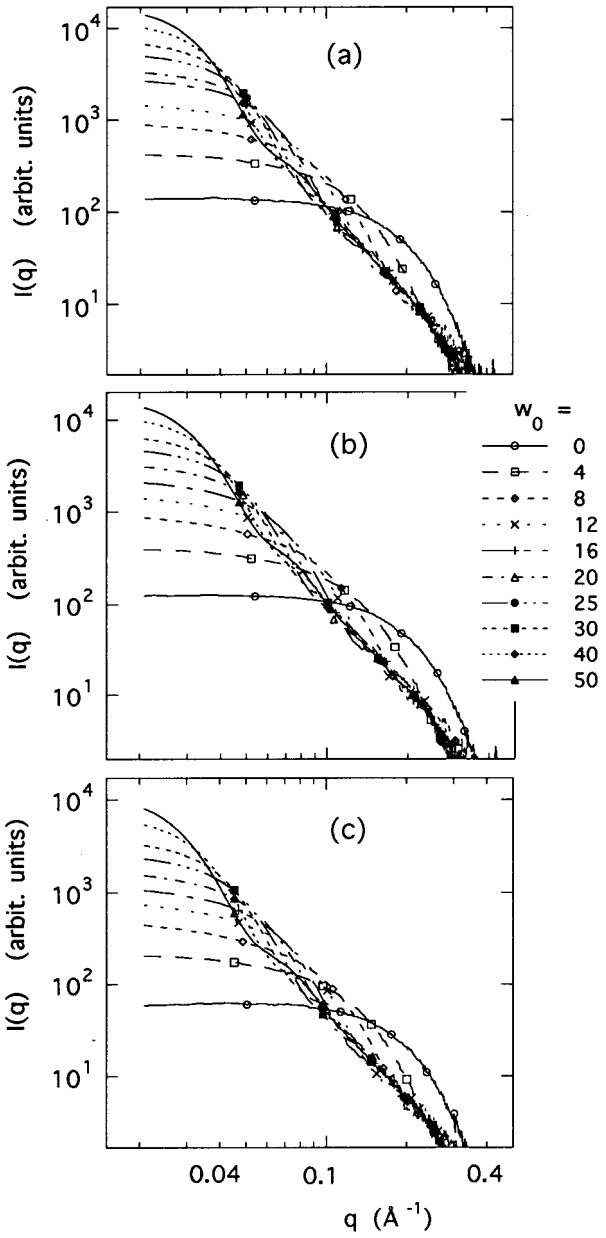

Figure 1. Scattering functions of 0.1 M AOT-reversed micellar solutions depending on water/surfactant molar ratio w_0 for different apolar solvents. Here, (a), (b), and (c) correspond to water/AOT/*n*-hexane, water/AOT/*n*-heptane, and water/AOT/*n*-octane systems, respectively.

characterize the relation of R_g vs w_0 by the slopes in the three different w_0 regions; that is, with increasing water content the three different regions with the different slopes appear successively. The slopes below $w_0 \leq 8$ are much larger than those above $w_0 \geq 12-20$, and between $8 \leq w_0 \leq 12-20$ the flat regions exist. R_g values estimated from SAXS data are *z*-averaged ones of all solute particle components. The *z*-averaged quantities are well known to be sensitive to high molar mass components, in other words, small amounts of relatively small particles should not significantly affect a *z*-average. This is the case in the appearance of the large slopes below $w_0 \leq 8$ in Figure 3. Combined with the results and discussion in Figures 2 and 5, at low water contents the presence of relatively large particles such as dimers or trimers should significantly increase the R_g value. As in the previous papers,[7,8,10] we will call these three different regions in w_0 dependence of R_g as oligomeric phase, transient phase, and monomeric phase, respectively. As

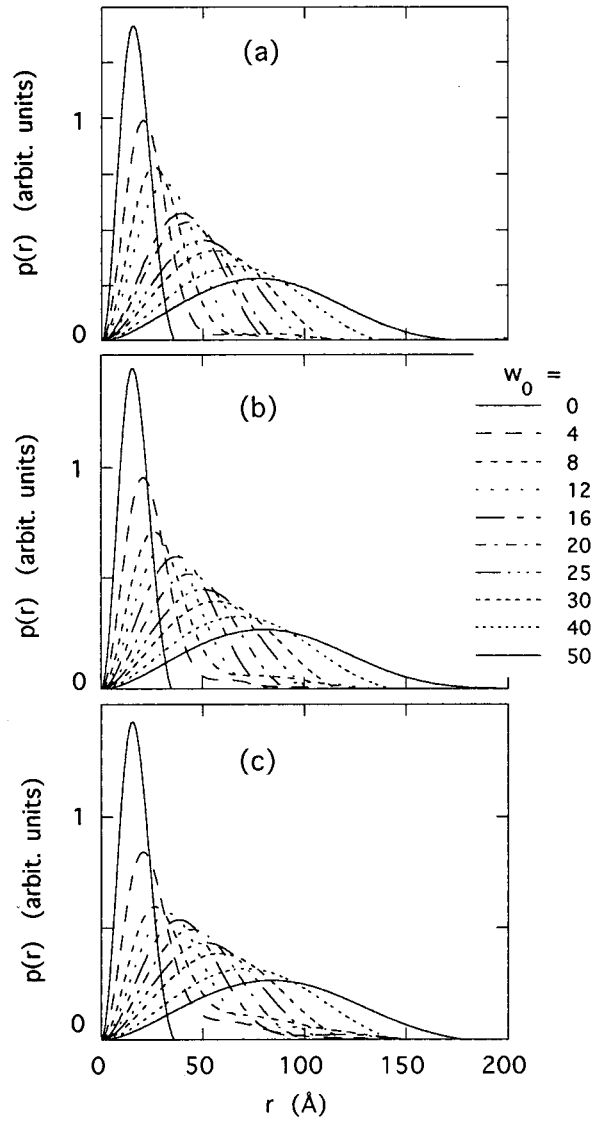

Figure 2. Distance distribution functions $p(r)$ of 0.1 M AOT-reversed micellar solutions depending on w_0 value for different apolar solvents. Here, (a), (b), and (c) are as in Figure 1.

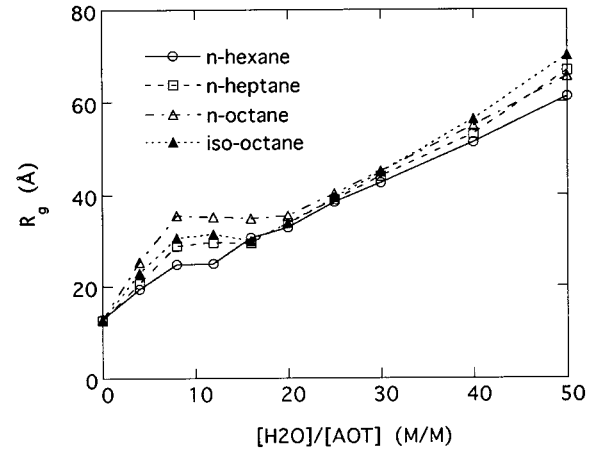

Figure 3. Dependence of radius of gyration of 0.1 M AOT-reversed micellar solutions on w_0 value for different apolar solvents. The marks correspond to the different AOT-reversed micellar solutions, namely ○, water/AOT/*n*-hexane; □, water/AOT/*n*-heptane; △, water/AOT/*n*-octane; ▲, water/AOT/isooctane.

suggested by the $p(r)$ functions, it should be noted that large oligomers would not exist even in the oligomeric phase at low water contents, namely, small amounts of relatively small oligomers would form and degenerate by collision between monomeric micelles. At $w_0 = 0$, the solution contains monomeric particles. The schematic pictures of those different phases are shown in Figure 4. On the other hand, except for the isooctane system, the slopes in Figure 3 mostly depend on the apolar solvents. The slopes at $w_0 \leq 8$ are 1.52 ± 0.09 for *n*-hexane, 2.04 ± 0.01 for *n*-heptane, 2.9 ± 0.2 for *n*-octane, and 2.2 ± 0.2 for isooctane. The slopes at $20 \leq w_0 \leq 50$ are 0.92 ± 0.02 for *n*-hexane, 1.07 ± 0.05 for *n*-heptane, 1.02 ± 0.04 for *n*-octane, and 1.30 ± 0.08 for isooctane. The w_0 range of the transient phase showing a flat relation of R_g vs w_0 is broadened systematically with the increase of the hydrocarbon chain length of the apolar solvent. Namely, the w_0 range of the transient phase is 8−12 for *n*-hexane, 8−16 for *n*-heptane and isooctane, and 8−20 for *n*-octane, indicating the transient region essentially depends on the hydrocarbon chain length.

In Figure 5 the w_0 dependence of the peak position p_{max} of the $p(r)$ function shows good linearity in the whole w_0 range. As shown previously,[13,14] not only for a monodispersed solution but also for a polydispersed solution containing oligomeric particles composed of identical globular particles, the first peak position p_{max} of the $p(r)$ function mostly corresponds to the radius of the constituent particle. Thus, the above good linearity indicates that for all AOT-reversed micellar systems measured the increase of water-pool radius is subject to a well-known,

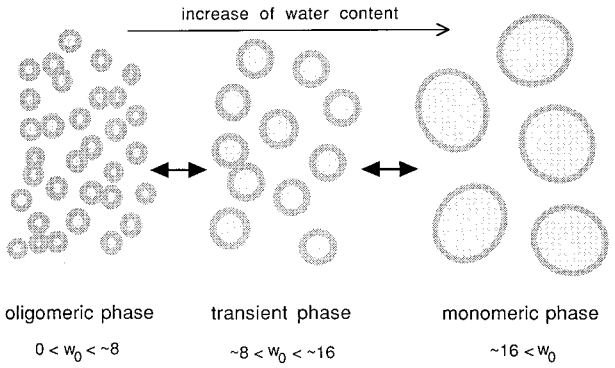

Figure 4. Schematic pictures of three different phases (oligomeric phase, transient phase, and monomeric phase) which appear successively with increasing water content. With shortening hydrocarbon chain length of apolar solvent, the presence probability of oligomeric particles at low water contents decreases and the phase boundaries shift to low water content. At $w_0 = 0$, every solution contains monomeric particles.

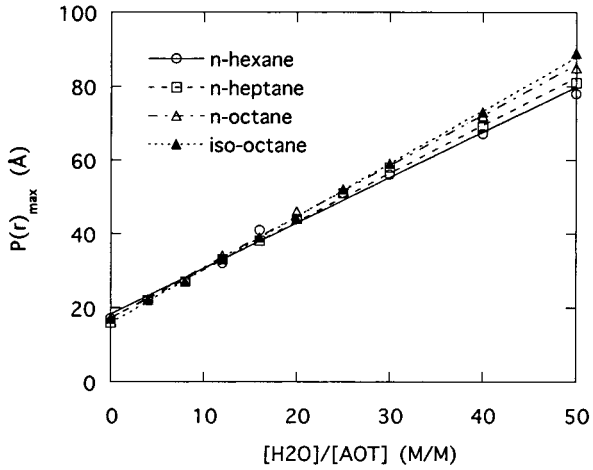

Figure 5. Plots of the peak position p_{max} of $p(r)$ function as the function of w_0 value for different apolar solvents. The marks correspond to the different AOT-reversed micellar solutions as shown in Figure 3.

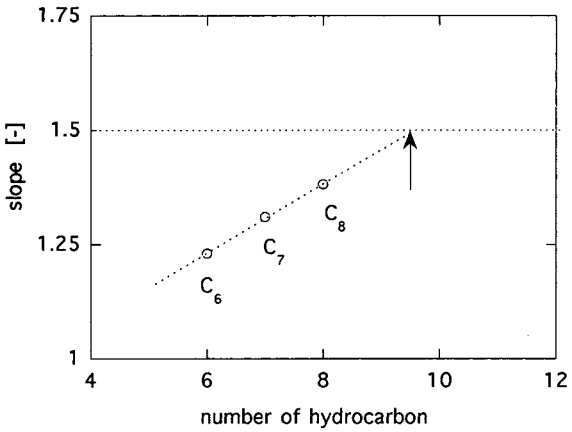

Figure 6. Plot of the slope of the linear relation between w_0 and p_{max} against the hydrocarbon chain length n_c. The slopes for different hydrocarbon chain lengths are obtained from the linear relations between w_0 and p_{max} in Figure 5.

simple linear relation between water-pool radius and w_0,[15,16] which is derived from geometric consideration of micellar packing of AOT molecules under composition constraints.[17−19] Namely, the water-pool radius R_w is simply given by $R_w = 3w_0V_w/\Sigma$, where V_w is the molecular volume of water and Σ is the area per polar headgroup of surfactant molecule. For AOT-reversed micelles, when we assume V_w and Σ are $\sim$30 Å^3 and $\sim$60 Å^2 respectively, $R_w = 1.5w_0$ Å is obtained.[20] According to the neutron scattering results, for an icosahedral packing of AOT polar heads at $w_0 = 0$, namely, for a dry AOT-reversed micelle, the micellar radius R was shown to be 16.4 Å.[21] Then R is turned out to satisfy $R = 1.5w_0 + 16.4$ Å. In our previous report where we studied the structure of the water/AOT/isooctane system with varying w_0 (0−50) and AOT concentration (0.05−0.2 M) at two different temperatures of 25 and 30 °C,[8] we showed the slopes of the plots of p_{max} against w_0 were 1.4−1.5. In the present AOT-reversed micellar systems, the slopes obtained from the linear least-squares fitting in the whole w_0 range in Figure 5 are 1.23 ± 0.04 for *n*-hexane, 1.31 ± 0.02 for *n*-heptane, 1.38 ± 0.02 for *n*-octane, and 1.44 ± 0.01 for isooctane, respectively. The last value for the isooctane system agrees well with our previous results and ensures the reproducibility of our SAXS experiments. Except for the isooctane system, we can recognize the dependence of the slope on the hydrocarbon chain length of the apolar solvent. Evidently the slope of 1.5 is derived from the assumption that the surfactant parameters are constant; therefore, the above systematic deviation of the experimental slopes from 1.5 is attributable to the distinctions of the apolar solvents. As is well known, the boiling temperatures of the apolar solvents are 69 °C for *n*-hexane, 98 °C for *n*-heptane, 126 °C for *n*-octane and 99 °C for isooctane, respectively, which reflect the strength of the intermolecular interaction between the apolar solvent molecules. In the present reversed micellar systems, if the interaction between the AOT polar head and water is assumed to be essentially unchanged, then the systematic deviation of the slopes from 1.5 would be explained by the penetration of apolar solvents into the nonpolar tail regions of the AOT surfactant layers. As predicted theoretically,[22] there is a penetration limit of apolar solvent which corresponds to the hydrocarbon chain length, and short chain apolar solvents penetrate easily into surfactant layers. In the case of reversed micellar systems, such penetrations enlarge the spontaneous curvature of the surfactant layer to reduce the micellar radius, which is clearly shown in Figure 5. In Figure 6 we plot the slope s of the linear relation between w_0 and p_{max} against the hydrocarbon chain length n_c. Although we used only three different apolar solvents with linear hydrocarbon chains, the extrapolation of the linear s vs n_c plot to the straight line of $s = 1.5$ gives an intersection at $n_c \sim 9.5$. This value would correspond to the penetration limit for AOT-reversed micellar systems under the present condition (at 25 °C under atmospheric pressure). Thus, the penetration of apolar solvents evidently reduces the reversed micellar radius.

On the other hand, the intercept values obtained from the linear least-squares fitting in Figure 5, corresponding to the micellar radii at $w_0 = 0$, are 16.5 ± 0.4 Å for *n*-hexane, 16.1 ± 0.2 Å for *n*-heptane, 16.4 ± 0.5 Å for *n*-octane, and 16.4 ± 0.3 Å for isooctane, respectively. Namely, within experimental error the radius of the dry AOT micelle does not show such a hydrocarbon chain length dependence, indicating that the icosahedral packing of the polar heads is a unique arrangement at $w_0 = 0$. Alternatively, this indicates that for the dry AOT-reversed micelles the radius is simply determined by the area per polar head Σ which is little affected by the penetration of apolar solvents.

Conclusion

We conclude the present findings as follows. As was previously reported for the water/AOT/isooctane system, with increasing water content the three different phases (oligomeric phase, transient phase, monomeric phase) appear successively for all systems, namely water/AOT/*n*-hexane, *n*-heptane, and *n*-octane systems. The w_0 region of the transient phase broadens with increasing the hydrocarbon chain length. Although the well-known linear relation between micellar radius and water content stands for all water/AOT/apolar solvent systems measured, the slope of the linear relation changes systematically depending on the length of the linear hydrocarbon chain of the solvent, which clearly suggests the penetration of the solvent molecules into the surfactant layer of the AOT-reversed micelle. The penetration limit of the solvent molecules into the surfactant layer can be estimated to be around 9.5 in number of hydrocarbon, so that over the linear hydrocarbon chain length of 9.5 the penetration of the apolar solvent molecules would hardly occur. In other words, with weakening the interaction between the apolar solvents the interpenetration of the solvents into the surfactant layer is enhanced to reduce the micellar radius, which results in the suppression of the appearance of oligomeric particles at low water content.

Acknowledgment. This work was performed under the approval of the Photon Factory Program Advisory Committee (Proposal No. 98G186 & 99P015).

References and Notes

(1) Bonner, F. J.; Wolf, R.; Luisi, P. L. *J. Solid-Phase Biochem.* **1980**, *5*, 255.
(2) Luisi, P. L.; Magid, L. J. *CRC Crit. Rev. Biochem.* **1986**, *20*, 409.
(3) Brochette, P.; Petitm, C.; Pileni, M. P. *J. Phys. Chem.* **1988**, *92*, 3505.
(4) Khmelnitsky, Y. L.; Kabanov, A. V.; Klyachko, N. L.; Levashov, A. V.; Martinek, K. In *Structure and Reactivity in Reversed Micelles*; Pileni, M. P. Ed.; Elsevier: Amsterdam, *1989*, p 230.
(5) Bru, R.; Walde, P. *Eur. J. Biochem.* **1991**, *199*, 95.
(6) Dorovska-Taran, V.; Veeger, C.; Visser, A. J. W. G. *Eur. J. Biochem.* **1993**, *218*, 1013.
(7) Hirai, M.; Hirai, R. K.; Nakamura, K.; Takizawa, T.; Yabuki, S.; Kobayashi, K.; Ameniya, Y.; Oya, M. *J. Chem. Soc., Faraday Trans.* **1995**, *91*, 1081.
(8) Hirai, M.; Hirai, R. K.; Nakamura, K.; Takizawa, T.; Yabuki, S.; Kobayashi, K.; Ameniya, Y.; Oya, M. *J. Phys. Chem.* **1995**, *99*, 6652.
(9) Hirai, R. K.; Hirai, M.; Iwase, H.; Arai, S.; Imai, M.; Matsushita, Y. *Physica B* **1998**, *241&243*, 984.

(10) Hirai, M.; Iwase, H.; Arai, S.; Mitsuya, S.; Hirai, R. K.; Takeda, T.; Seto, H.; Nagao, M. *J. Phys. Chem. Solids* **1999**, *60*, 1359.

(11) Ueki, T.; Hiragi, Y.; Kataoka, M.; Inoko, Y.; Amemiya, Y.; Izumi, Y.; Tagawa, H.; Muroga, Y. *Biophys. Chem.* **1985**, *23*, 115.

(12) Glatter, O. In *Small-Angle X-ray Scattering*; Glatter, O., Kratky, O., Eds. Academic Press: London, 1982, p 119.

(13) Hirai, M.; Hirai, R. K.; Hirai, T.; Ueki, T. *Eur. J. Biochem.* **1993**, *215*, 55.

(14) Hirai, M.; Iwase, H.; Arai, S.; Takizawa, T.; Hayashi, K. *Biophys. J.* **1998**, *74*, 1380.

(15) Pileni, M. P.; Zemb, T.; Petit, C. *Chem. Phys. Lett.* **1985**, *118*, 414.

(16) Pileni, M. P. *J. Phys. Chem.* **1993**, *97*, 6961.

(17) Israelachvili, J. N.; Mitchell, D. J.; Ninham, B. W. *J. Chem. Soc., Faraday Trans. 2* **1976**, *72*, 1525.

(18) Israelachvili, J. N.; Mitchell, D. J.; Ninham, B. W. *Biochim. Biophys. Acta* **1977**, *470*, 185.

(19) Mitchell, D. J.; Ninham, B. W. *J. Chem. Soc., Faraday Trans. 2* **1981**, *77*, 601.

(20) Langevin, D. In *Structure and Reactivity in Reversed Micelles*; Pileni, M. P. Ed.; Elsevier: Amsterdam, 1989, p 13.

(21) Katlarchyk, M.; Huang, J. S.; Chen, S. H. *J. Chem. Phys.* **1985**, *89*, 4382.

(22) Gruen, D. W. R.; Haydon, D. A. *Pure Appl. Chem.* **1980**, *52*, 1229.